Annals of Botany **122**: 227–238, 2018
doi: 10.1093/aob/mcy047, available online at www.academic.oup.com/aob

ANNALS OF BOTANY
Founded 1887

The maize *lilliputian1* (*lil1*) gene, encoding a brassinosteroid cytochrome P450 C-6 oxidase, is involved in plant growth and drought response

Giulia Castorina[1], Martina Persico[1], Massimo Zilio, Stefano Sangiorgio, Laura Carabelli and Gabriella Consonni*

Department of Agricultural and Environmental Sciences - Production, Landscape, Agroenergy (DISAA), Università degli Studi di Milano, Via Celoria 2, 20133 Milan, Italy
**For correspondence. E-mail gabriella.consonni@unimi.it*
[1]*Both authors contributed equally to this work.*

Received: 22 February 2018 Returned for revision: 2 January 2018 Editorial decision: 5 March 2018 Accepted: 13 March 2018
Published electronically 16 May 2018

• **Background and Aims** Brassinosteroids (BRs) are plant hormones involved in many developmental processes as well as in plant–environment interactions. Their role was investigated in this study through the analysis of *lilliputian1-1* (*lil1-1*), a dwarf mutant impaired in BR biosynthesis in maize (*Zea mays*).
• **Methods** We isolated *lil1-1* through transposon tagging in maize. The action of *lil1* was investigated through morphological and genetic analysis. Moreover, by comparing *lil1-1* mutant and wild-type individuals grown under drought stress, the effect of BR reduction on the response to drought stress was examined.
• **Key Results** *lil1-1* is a novel allele of the *brassinosteroid-deficient dwarf1* (*brd1*) gene, encoding a brassinosteroid C-6 oxidase. We show in this study that *lil1* is epistatic to *nana plant1* (*na1*), a BR gene involved in earlier steps of the pathway. The *lill-1* mutation causes alteration in the root gravitropic response, leaf epidermal cell density, epicuticular wax deposition and seedling adaptation to water scarcity conditions.
• **Conclusions** Lack of active BR molecules in maize causes a pleiotropic effect on plant development and improves seedling tolerance of drought. BR-deficient maize mutants can thus be instrumental in unravelling novel mechanisms on which plant adaptations to abiotic stress are based.

Key words: Brassinosteroids, *brassinosteroid-deficient dwarf1* (*brd1*), cell density, cuticular waxes, CYP85A, drought stress, dwarf mutant, gravitropic response, *lilliputian1* (*lil1*), *nana plant1* (*na1*), P450 C-6 oxidase, *Zea mays*.

INTRODUCTION

Brassinosteroids (BRs) are a class of steroid hormones essential for plant growth and development (Clouse, 2011). They control cell elongation, division and differentiation and are also involved in the control of many developmental traits of agronomic importance, such as seed germination, leaf curvature, flowering time and seed yield (Divi and Krishna, 2009; Vriet *et al.*, 2012).

Several BR biosynthetic steps have been unravelled through the study of mutants, the main features of which are reduced stature and the presence of round and dark green leaves. Castasterone (CS) and brassinolide (BL), the two active BR molecules, are produced in the final steps of the BR pathway by members of the CYP85A family of cytochrome P450 monooxygenases. The isolation of their corresponding genes was first achieved in tomato (*Lycopersicon esculentum*) through the molecular characterization of two extreme dwarf mutants. The tomato *Dwarf* gene, encoding LsCYP85A1, which catalyses the C-6 oxidation of 6-deoxo castasterone (6-deoxoCS) to CS, is expressed in the vegetative part of the plant (Bishop *et al.*, 1996, 1999). *LsCYP85A3*, involved in the conversion of CS to BL, is preferentially expressed in fruits (Nomura *et al.*, 2005). Analogously, two *AtCYP85A* genes involved in the final reactions of BR biosynthesis were detected in *Arabidopsis thaliana*. AtCYP85A2 is specifically involved in the CS-to-BL conversion (Nomura *et al.*, 2005) while AtCYP85A1 catalyses the C-6 oxidation reactions of multiple substrates (Shimada *et al.*, 2001). Mutations in the *AtCYP85A2* gene result in severe dwarfism, whereas *Atcyp85a1* mutations do not affect plant development, but cause failure of female gametogenesis (Pérez-España *et al.*, 2011). Unlike what has been reported in dicot species, studies in monocots reported a single CYP85A gene. The *OsCYP85A1/OsBRD1* and *Zmbrd1* genes, both encoding a BR C6-oxidase, were isolated in rice (*Oryza sativa*) (Kim *et al.*, 2008) and maize (*Zea mays*) (Makarevitch *et al.*, 2012), respectively.

In maize, two additional genes involved in BR biosynthesis, i.e. *nana plant1* (*na1*) and *nana plant2* (*na2*), have been isolated. The *na1* gene, encoding a 5α-reductase enzyme (Hartwig *et al.*, 2011), is the homologue of the *A. thaliana* gene *DEETIOLATED2* (*DET2*) (Li *et al.*, 1996) , while *na2*, encoding a D24-sterol reductase (Best *et al.*, 2016), corresponds to *DWARF1* in *A. thaliana* (Choe *et al.*, 1999). Moreover, the maize BR receptor BRASSINOSTEROID INSENSITIVE1 (BRI1) has been characterized by using a transgenic RNA interference (RNAi) approach that knocked down the expression of all five maize *BRI1* homologous genes (Kir *et al.*, 2015). The resulting mutant phenotype includes dwarf stature, due to

shortened internodes, dark green, upright, and twisted leaves with decreased auricle formation, and feminized male flowers.

So far, mutant studies conducted in maize have focused on the role of BRs in developmental processes. However, there is growing evidence that mutants with deficiencies either in the synthesis or the perception of BR are instrumental for unravelling the role of these hormones in the interactions between plant and environment (Feng *et al.*, 2015; Gruszka *et al.*, 2016). Data obtained in this context will have important implications in crop breeding since genetic manipulation of the BR level could improve plant tolerance to environmental stresses.

Here we report the characterization of *lil1-1*, a novel allele at the maize *brd1* locus. A mutant allele at this locus, referred to as *brd1-m1*, was previously isolated in a population mutagenized with ethyl methanesulfonate (EMS). Molecular characterization of *brd1-m1* revealed the presence of single base-pair substitution resulting in the creation of a premature stop codon and thus generating a truncated protein (Makarevitch *et al.*, 2012).

We detected some peculiar traits in the *lil1-1* mutant, such as altered root gravitropic response and epicuticular wax deposition. We also analysed the genetic interaction between *lil1-1* and the *na1-1* mutant, which is impaired in earlier steps of biosynthesis and exhibits a less severe phenotype. Moreover, by comparing *lil1-1* mutant and wild-type individuals, we examined the effect of BR reduction on the response to drought stress during early phases of plant development.

MATERIALS AND METHODS

Plant materials and growth conditions

The maize (*Zea mays*) *lil1-1* mutant was originally isolated from the selfed progeny of a *Mutator* stock outcrossed to an unrelated stock (Dolfini *et al.*, 1999). The *lil1-1* mutant allele was introgressed into B73, A188, H99 and *Rsc-m2* inbred lines. The *brd1-m1* (Makarevitch *et al.*, 2012) and *na1-1* (Hartwig *et al.*, 2011) mutant lines were obtained from the Maize Genetics Cooperation Stock Center. Due to impaired inflorescence development, mutant plants were maintained as heterozygotes. In all the experiments performed, homozygous mutants and their wild-type control plants were from the same F_2 segregating progeny.

Plants were grown in a growth chamber with controlled temperature (25 °C night, 30 °C day) and under a long-day photoperiod (16 h of light/8 h of dark) with photon fluence of 70 µmol m^{-2} s^{-1}. For phenotypic analysis at the seedling level, seeds were germinated and grown for 10 days on wet filter paper; for analysis at later developmental stages, plants were grown on soil.

Cloning of lil1 *and transcript analysis*

Co-segregation analysis was performed on DNA samples extracted from single-mutant (*lil1-1/lil1-1*) and wild-type plants, whose homozygous (+/+) or heterozygous (+/*lil-1*) constitution was ascertained through self-pollination. Genomic DNA extraction and Southern analysis were performed as previously described (Gutiérrez-Marcos *et al.*, 2007). Hybridization probes were as follows: the *Mu1*-specific probe corresponded to the AvaI/BstNI 650-bp central fragment of the *Mu1* element; the *lil1*-specific probe was the EcoRV/SalI 443-bp fragment obtained from the genomic region flanking the *Mu1* insertion. The genomic fragment co-segregating with the lil1 mutant phenotype was cloned by the screening of a size-fractionated EcoRI library of genomic DNA with the *lil1* probe. For PCR-based co-segregation analysis, genomic DNA was extracted as previously described (Arthur *et al.*, 2003).

For reverse-transcription (RT) PCR, total RNA was extracted with TRIzol reagent following the manufacturer's instructions (Thermo Fisher Scientific). DNase treatment was performed with the reagent RQ1 RNase-Free DNase (Promega) and first-strand cDNA was synthesized from 750 ng of RNA using a High-Capacity cDNA Reverse Transcription Kit (Thermo Fisher Scientific).

Genomic DNA and cDNA were subjected to amplification with GoTaq® Flexi DNA Polymerase (Promega), and PCRs were conducted with different sets of primers (Supplementary Data Table S6).

Allelism test

Pollen of a given +/*brd1-m1* plant, whose heterozygous condition was ascertained by selfing, was applied to the silks of +/*lil1-1* plants, whose heterozygous condition was determined by PCR analysis. F_1 seeds were germinated to score the seedling phenotypes. About one-quarter of seedlings are expected to be mutant if there is lack of complementation (allelism). Statistical analysis was conducted using the χ^2 test to confirm the observed segregation.

Microscopy analyses

To obtain histological images of the shoot apical meristem (SAM), 2-week-old homozygous *lil1-1* and wild-type plants were sampled from the same segregating progeny grown under standard conditions in the growth chamber. Shoot tissues were immediately fixed in 3 % glutaraldehyde in phosphate-buffered saline (PBS) (130 mM NaCl, 7 mM Na_2HPO_4, 3 mM NaH_2PO_4) for 24 h. The fixed material was placed in 70 % ethanol and embedded in LR White resin. Semi-thin sections (2 µm) were applied to polylysine-coated slides, stained with Toluidine Blue O [1 % toluidine blue 1 % sodium tetraborate (1:1, v/v)] and imaged under a light microscope (Ortholux, Leitz, Germany). Leaf-blade samples were fixed with 3 % glutaraldehyde in PBS and then embedded in 5 % agar. Sections of 30 µm were cut with a microtome.

For the analysis of epicuticular waxes, leaf pieces of wild-type and *lil1-1* mutant plants were dried and processed according to La Rocca *et al.* (2015). The specimen surfaces were examined with a SEMLEO 1430 (Zeiss) microscope.

Phenotypic analysis

Mesocotyl, coleoptile, primary root length and seedling height, measured from the scutellar node to the tip of the last emerging leaf, were determined on a sample of 20 plants per genotype. Data are reported as the mean ± standard error.

Pairwise comparisons between means of the two genotypes were performed using a two-tailed Student's *t*-test.

Plant height analysis in the progeny segregating for *lil1-1* and *na1-1* alleles was performed for a sample of 102 wild-type, 31 homozygous *na1-1*, 26 homozygous *lil1-1* and 12 double-homozygous *na1-1 lil1-1* seedlings. A one-way ANOVA test was performed with the statistical package SPSS 21.0.

Cell density and stomatal index analysis

To measure stomatal density and stomatal index, a leaf surface imprint method was used. We analysed the fourth and sixth fully expanded leaves of ~50-day old mutant and wild-type plants. Briefly, a thin film of vinyl glue (SuperVinil) was applied with a small paintbrush on both the adaxial and the abaxial surface of the median portion of the leaf still attached to the plant, in order to prevent wilting. One imprint per leaf was taken from a minimum of eight independent plants for wild-type, *na1-1* or *lil1-1* and four independent plants for *lil1-1 na1-1* genotypes. The imprints were then put on glass microscope slides and observed under a light microscope (DM RA2 optical microscope, Leica, Wetzlar, Germany) at 10× magnification. Two viewable leaf areas (0.807 mm^2) between vascular tissues were randomly selected per imprint and photographed. The total numbers of stomata and pavement cells were determined by counting all the cells in each area and mean parameters were calculated. The stomatal index was determined as [number of stomata/(number of epidermal cells + number of stomata)] × 100. A one-way ANOVA test was performed with the statistical package SPSS 21.0.

Chlorophyll leaching analysis

Completely expanded sixth leaves were taken from five independent plants per genotype and dissected into pieces of 8-cm length measured from the apex. Leaf sectors were weighed, immersed in 80 % ethanol and incubated at room temperature. Every vial was carefully covered to protect the samples from light. A series of 1-mL aliquots were taken at 12, 24, 36, 48, 60 and 72 h. Absorbance was measured at 647 and 664 nm with a spectrophotometer (Agilent Technologies Cary 60 UV-Vis) to quantify the chlorophyll released in the solution. The micromolar concentration of total chlorophyll per gram of fresh weight (FW) of tissue was calculated using the equation described by Lolle *et al.* (1997): total micromoles of chlorophyll = 7.93 (A_{664}) + 19.53 (A_{647}).

Plant growth conditions in drought stress and recovery experiments

For the drought stress experiment, seedlings at the coleoptile developmental stage were transferred to pots (8 × 8 cm) containing SER V8-14L substrate (Vigorplant, Piacenza, Italy). Each pot contained one seedling and the same amount of soil. To monitor the drought stress level, the relative soil water content (RSWC) was measured throughout the experiment. First, the maximum soil water content (RSWC = 100 %) was determined (Janeczko *et at.* 2016). The pots were watered until complete imbibition, left to lose the water excess and then weighed (wet weight). Subsequently, the soil was completely dried out at 60 °C for 5 days (dry weight). The 100 % RSWC was calculated as wet weight minus dry weight. All plants were grown under the well-watered condition (RSWC = 70 %) until the fourth leaf was emerging, and on the next day (Day 0) drought stress was initiated by withholding irrigation. The RSWC were measured at 0, 3, 6 and 9 days from the start of the drought treatment. At each time point there were 20 pots per genotype.

For the recovery assay, 9 days after the beginning of the drought treatment, 40 plants of each genotype were re-watered and after 3 and 7 days from re-watering were classified on a visual scale into three categories: 1 (severely wilted); 2 (slightly wilted); and 3 (recovered). The data collected for each category were expressed as percentage of the total number of tested plants.

Determination of leaf relative water content

To determine the leaf relative water content (RWC), discs 7 mm in diameter were taken from the widest portion of the fourth leaf at 0 and 9 days after the cessation of irrigation.

After fresh weight determination, the discs were floated in Petri dishes with distilled water for 24 h at room temperature. Following surface drying with absorbent paper towels and turgid weight determination, the discs were oven-dried at 37 °C for 4 days and reweighed to determine the dried weight. The leaf RWC was calculated as (fresh weight – dry weight)/(turgid weight – dry weight) × 100 (Pieczynski *et al.*, 2013). Leaves were from ten individual plants per genotype and two discs were taken from each leaf. The average was calculated, and pairwise comparison between the two genotypes was performed using a two-tailed Student's *t*-test.

Leaf gas exchange analysis

Measurements of gas exchange were made at 0, 3 and 4 days after the cessation of irrigation, with a portable open-system infra-red gas analyser (CIRAS-2, PP Systems, Hitchin, UK). Measurements were made on portions of leaf lamina of 1.7 cm^2, with an air flow rate of 300 mL min^{-1}, at a photosynthetic photon flux density (PPFD) of 1000 µmol m^{-2} s^{-1}. The ambient temperature was 35–38 °C and the vapour pressure deficit (VPD) was similar during the whole experiment. Measurements were taken three times for each plant. Stomatal conductance (g_s), transpiration rate (E), intercellular CO_2 (C_i) and net photosynthesis rate (A) were directly retrieved from CIRAS-2 measurements. Water use efficiency (WUE) was calculated as the ratio between A and E. Physiological parameters were measured on well-developed fourth leaves in five replicates/genotype, where one replicate represented one leaf from an individual plant. Pairwise comparisons between means of different genotypes were performed using a two-tailed Student's *t*-test.

RESULTS

The maize lil1-1 *mutant is a novel allele of the* brd1 *gene*

The *lil1-1* recessive mutant was isolated from an active *Mutator* (*Mu*) stock (Dolfini *et al.*, 1999). Genomic sequences associated with the *lil1* mutant phenotype were identified

through a Southern-based co-segregation analysis. In this analysis, genomic DNA was extracted from 40 wild-type (+/*lil1-1* and +/+) and 20 mutant (*lil1-1*/*lil1-1*) single individuals and cut with the EcoRI restriction enzyme. Hybridization with a *Mu1*-specific probe revealed the presence of a polymorphic restriction fragment, of ~9.5 kb, co-segregating with the mutant allele (Supplementary Data Fig. S1A). Cloning and subsequent sequencing of the fragment confirmed the presence of a *Mu1* element and disclosed the presence of a genomic region flanking the transposon insertion. To verify the identity of the cloned fragment, the same EcoRI-digested DNA blot was hybridized with a probe obtained from the flanking sequence. Individuals carrying the *lil1-1* allele showed the same 9.5 Kb fragment (Supplementary Data Fig. S1B). A PCR-based co-segregation analysis was also performed and showed absence of recombination between the *lil1* phenotype and the *Mu1* insertion on a sample of a total of 100 F_2 individuals, thus indicating a correspondence between this insertion and the *lil1-1* mutant allele (Supplementary Data Fig. S1C). BLAST analysis of the cloned region flanking the *Mu1* insertion showed complete homology with the *brd1* gene (GRMZM2G103773) encoding a cytochrome P450 CYP85A1 C-6 oxidase (CYP85A1) (Makarevitch *et al.*, 2012). In the *lil1-1* allele the *Mu1* element was inserted in the second exon of the *brd1* gene (Fig. 1A). RT–PCR analysis was also performed to compare wild-type and mutant transcripts (Supplementary Data Fig. S1C). Results obtained with the Lil1F4-Lil1R5 primer set showed that the CYP85A1 transcript accumulates in wild-type as well as in *lil1-1* and *brd1-1* mutants. An amplification product of the expected size was specifically detected with the Lil1F5-Mu53 primer set in the *lil1-1* mutant, while the Lil1F5-Lil1R3 set of primers spanning the *Mu1* insertion gave an amplification product only in wild-type and *brd1-1* mutant DNAs. This indicates that the *lil1-1* mutant transcript retained the *Mu1* element. This aberrant transcript is thus predicted to encode a non-functional protein.

The *lil1-1* allele was indistinguishable from the previously isolated *brd1-m1* allele (Makarevitch *et al.*, 2012), since both exhibited an obvious and similar dwarf seedling phenotype, which was clearly distinguishable from that of wild-type seedlings (Fig. 1B, Supplementary Data Fig. S2). To confirm that *lil1-1* and *brd1-m1* mutants were ascribable to the same gene an allelism test was done. Heterozygous +/*lil1-1* female plants, the genotype of which had been determined by PCR analysis, were crossed to +/*brd1-m1* plants, whose genotype was ascertained by self-pollination. The mutant segregation value observed in the progeny confirmed that the two mutants are allelic (Supplementary Data Table S1), thus providing a further proof of *lil1* gene identity.

The lil1-1 *mutation has a pleiotropic effect on plant growth*

Involvement of BRs in seed production has been shown in studies conducted in arabidopsis and rice (Vriet *et al.*, 2012). However, lack of *lil1* activity does not appear to have an effect on the maize kernel. No visible defects were present at morphological level and no difference in weight was detected between *lil1-1* mutant and wild-type seeds, whose genotypes were ascertained through germination (Supplementary Data Table S2). We also excluded the possibility that the *lil1* constitution of the mother plant affects seed production. Seed weight and number were compared in F_2 progeny ears obtained from selfing either F_1 heterozygous or homozygous wild-type plants. In most of the lines, segregating and non-segregating ears did not differ in seed weight. Similarly, seed number per ear did not differ between segregating and non-segregating ears (Supplementary Data Table S3).

The effects of the *lil1-1* mutation on plant growth were analysed in more detail. Segregating F_2 progenies were obtained by introgressing the mutation in different genetic backgrounds. The *lil1-1* mutant allele was introgressed three times in B73 and once in *R-scm2*, H99 and A188 genetic backgrounds. At 10 days after sowing, homozygous *lil1-1* mutant seedlings showed the same phenotype in all backgrounds tested. Mutant mesocotyl elongation was blocked, and mutant coleoptile elongation was ~25 % of that of the wild type (Table 1).

Reduced elongation of mutant compared with wild-type leaf primordia was also observed in histological analysis of shoot apices (Fig. 2A, B). Mutant leaves, at later developmental stages, exhibited an altered shape, visible in blade transverse sections. They also appeared thicker (Fig. 2D) than wild-type leaves (Fig. 2C) and presented supernumerary cell layers in the mesophyll region between leaf vessels and the leaf epidermis (Fig. 2D).

Primary root elongation was also significantly reduced in comparison with wild type (Supplementary Data Fig. S2A, C) and this was observed in all the different lines tested (Table 1). Interestingly, seedlings germinated on wet filter paper showed altered root gravitropic curvature. Mutant roots grew either upwards or parallel to the surface (Fig. 2E, F, Supplementary Data Fig. S2A). A positive gravitropic response (Fig. 2G) was instead observed in all wild-type seedlings analysed (Supplementary Data Table S4). The mutant-specific root phenotypes were detected in all genetic backgrounds tested (Supplementary Data Table S4) and was also observed in *brd1-m1* mutants (Supplementary Data Fig. S2A). We thus conclude that lack of active BR molecules does not interfere with seed formation in maize but causes a pleiotropic effect on plant development.

The lil1-1 *mutant is epistatic to the* na1-1 *mutant*

The *na1-1* (Hartwig *et al.*, 2011) and *lil1-1* mutants are impaired in the earlier and the final steps of the BR biosynthesis, respectively. We observed that in homozygous *na1-1* (*na1-1*/*na1-1*) plants growth defects appeared less severe than in homozygous *lil1-1* (*lil1-1*/*lil1-1*) plants. Therefore, to compare their phenotypes as well as to analyse the genetic relationship between the two mutants, F_2 progenies were produced from selfing heterozygous na1-1/+ lil1-1/+ F_1 plants. A first analysis was performed at the seedling developmental stage through visual scoring of F_2 plant phenotypes. Three phenotypic classes were detected, comprising the wild-type class and two distinct mutant classes, referred to as ‘na1-1 like’ and ‘lil1-1 like’, respectively (Fig. 3A). The latter exhibited the most severe phenotype and the more severe reduction in shoot elongation (Fig. 3A). When tested for fit

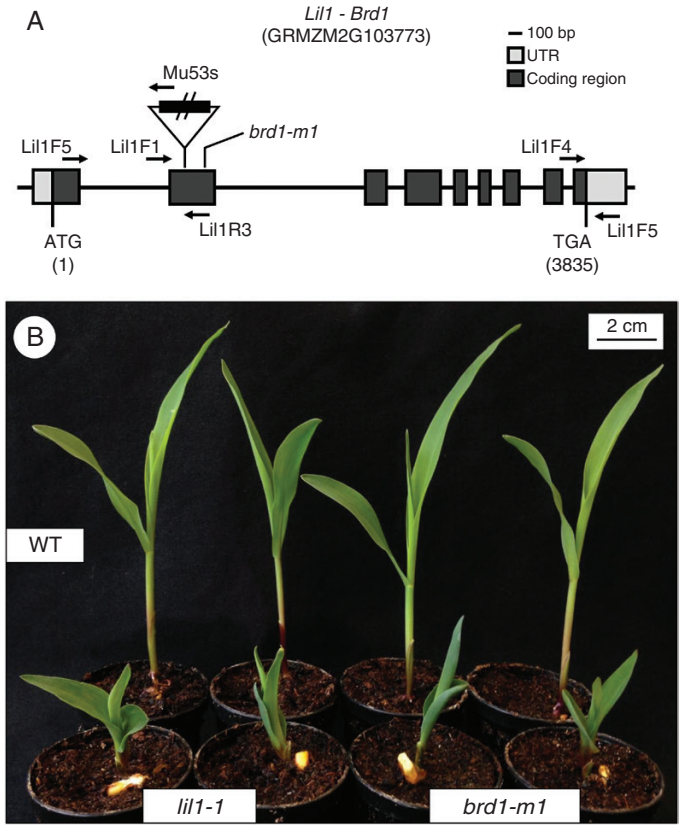

FIG. 1. The *lil1-1* mutant is an allele of *brd1*. (A) Schematic representation of the maize *cytochrome P450 CYP85A1* C-6 oxidase gene structure (Maize B73 RefGen_v3). The *lil1-1* mutant allele carries a *Mutator1* (*Mu1*) insertion, indicated as a triangle, in the second exon at 877 bp from the ATG start codon. Positions of the *brd1-m1* mutation at 1145 bp (Makarevitch *et al.*, 2012) and of primers (arrows) used in this work are also indicated. (B) Representative phenotypes of 10-day old wild-type, homozygous *lil1-1* and homozygous *brd1-m1* seedlings. Scale bar = 2 cm.

TABLE 1. *Morphometric analysis of homozygous* lil1-1 *mutant and wild-type (WT) seedlings in four different genetic backgrounds. Standard error is reported (±). All measured differences between homozygous* lil1-1 *mutant and wild-type plants were statistically significant (*P < *0.001, two-tailed Student's* t*-test)*

Genetic background	Seedling height (cm)		Mesocotyl length (cm)		Coleoptile length (cm)		Root length (cm)	
	lil1-1	WT	*lil1-1*	WT	*lil1-1*	WT	*lil1-1*	WT
B73	3.70 ± 0.39	13.02 ± 0.73	0.04 ± 0.04	0.94 ± 0.05	0.66 ± 0.11	2.59 ± 0.08	11.52 ± 0.89	16.07 ± 1.12
R-scm2	3.40 ± 0.29	11.84 ± 0.85	0.00 ± 0.00	0.99 ± 0.15	0.77 ± 0.12	2.83 ± 0.08	8.75 ± 0.80	13.72 ± 1.29
H99	5.34 ± 0.39	18.93 ± 0.66	0.00 ± 0.00	0.59 ± 0.05	0.59 ± 0.05	2.57 ± 0.11	12.60 ± 1.50	23.80 ± 0.99
A188	4.27 ± 0.33	15.20 ± 0.60	0.00 ± 0.00	0.44 ± 0.04	0.62 ± 0.06	2.08 ± 0.11	12.71 ± 0.97	22.14 ± 0.93

to a 9:3:4 segregation ratio, the calculated χ^2 value (0.9142) confirmed the segregation hypothesis (Supplementary Data Table S5). The genotype of single individuals was then determined through PCR analysis (see the Materials and methods section). The analysis confirmed the presence of four genotypic classes along with the 9:3:3:1 segregation ratio expected ($\chi^2 = 1.6939$). It also showed that individuals homozygous for *na1-1* (*na1-1/na1-1 Lil1/−*) were all included in the na1-like mutant class while both homozygous *lil1-1* (*Na1/− lil1-1/lil1-1*) and double-homozygous *na1-1 lil1-1* (*na1-1/na1-1 lil1-1/lil1-1*) mutant seedlings belonged to the lil1-like category (Supplementary Data Table S5). This classification was maintained at later developmental stages (Supplementary Data Fig. S3A–D). Wild-type plants (Supplementary Data Fig. S3A) were clearly distinguishable from mutant plants (Supplementary Data Fig. S3B–D). Homozygous *na1-1* plants (Supplementary Data Fig. S3B) were recognizable for their erect leaves (Hartwig *et al.*, 2011). Homozygous *lil1-1* (Supplementary Data Fig. S3C) and double-homozygous *na1-1 lil1-1* (Supplementary Data Fig. S3D) mutant plants were phenotypically identical and showed a drastic reduction in growth compared with both wild-type and homozygous *na1-1* plants. Analysis of the four genotypic classes for seedling height showed that their mean values were statistically different except for *lil1-1* and *na1-1 lil1-1* plants, which did not differ from each other (Fig. 3B). Overall these data confirmed

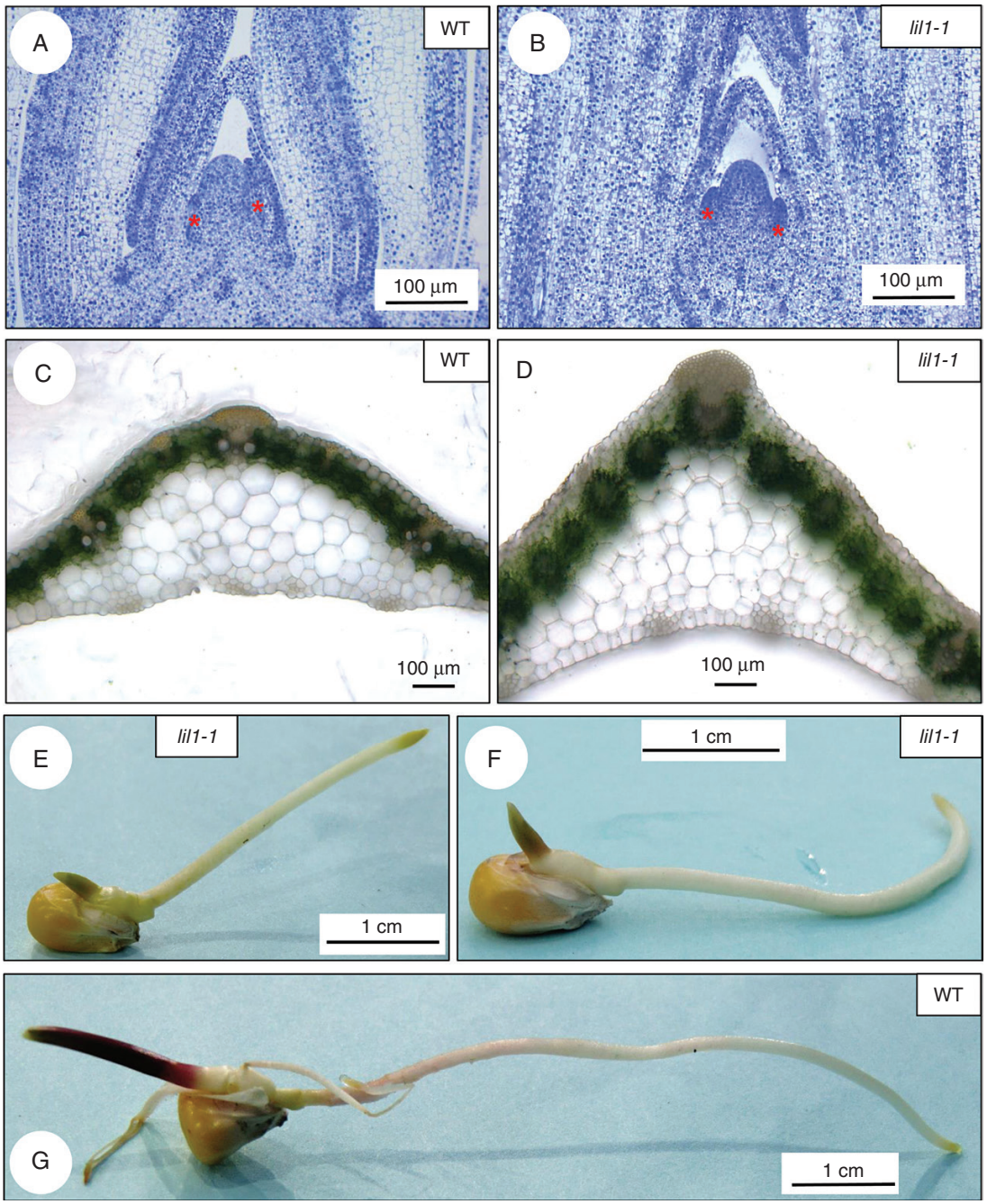

FIG. 2. Morphological features of *lil1-1* mutants. (A, B) Longitudinal sections of shoot apices of 2-week-old wild-type (A) and homozygous *lil1-1* mutant (B) plants. Samples were stained with Toluidine Blue O. Red asterisks mark leaves primordia. (C, D) Transverse section of leaf blades of 2-week-old wild-type (C) and homozygous *lil1-1* mutant (D) plants. (E–G) Primary root of 4-day old seedlings. Altered gravitropic response in homozygous *lil1-1* mutant roots growing upwards (E) or parallel to the surface (F) compared with wild-type (WT) root, which shows a positive gravitropic response (G).

that the lil1 phenotype is more severe than the na1 phenotype and showed that *lil1* is epistatic to *na1*.

The genetic relationship between *na1* and *lil1* was also investigated for epidermal traits. The cell density and stomatal index were analysed in the median portion of fully expanded fourth and sixth leaves (Fig. 3, Supplementary Data Fig. S3).

Comparison of the cell density in the fourth leaf adaxial side (Fig. 3C) among wild-type, single and double mutant plants revealed that both single homozygous *na1-1* and *lil1-1* mutants have a higher density of pavement cells (PCs) compared with wild type. Analogously to seedling height (Fig. 3B), single homozygous *lil1-1* and double homozygous *lil1-1 na1-1* mutants showed a higher PC density compared with *na1-1* (Fig. 3C). With regard to guard cell (GC) density, that of the wild type was lower and significantly different from that of all single and double mutants (Fig. 3C). Moreover, in plants carrying the *lil1-1* mutation in homozygous state the stomata appeared unevenly distributed (Supplementary Data Fig. S3G, H)

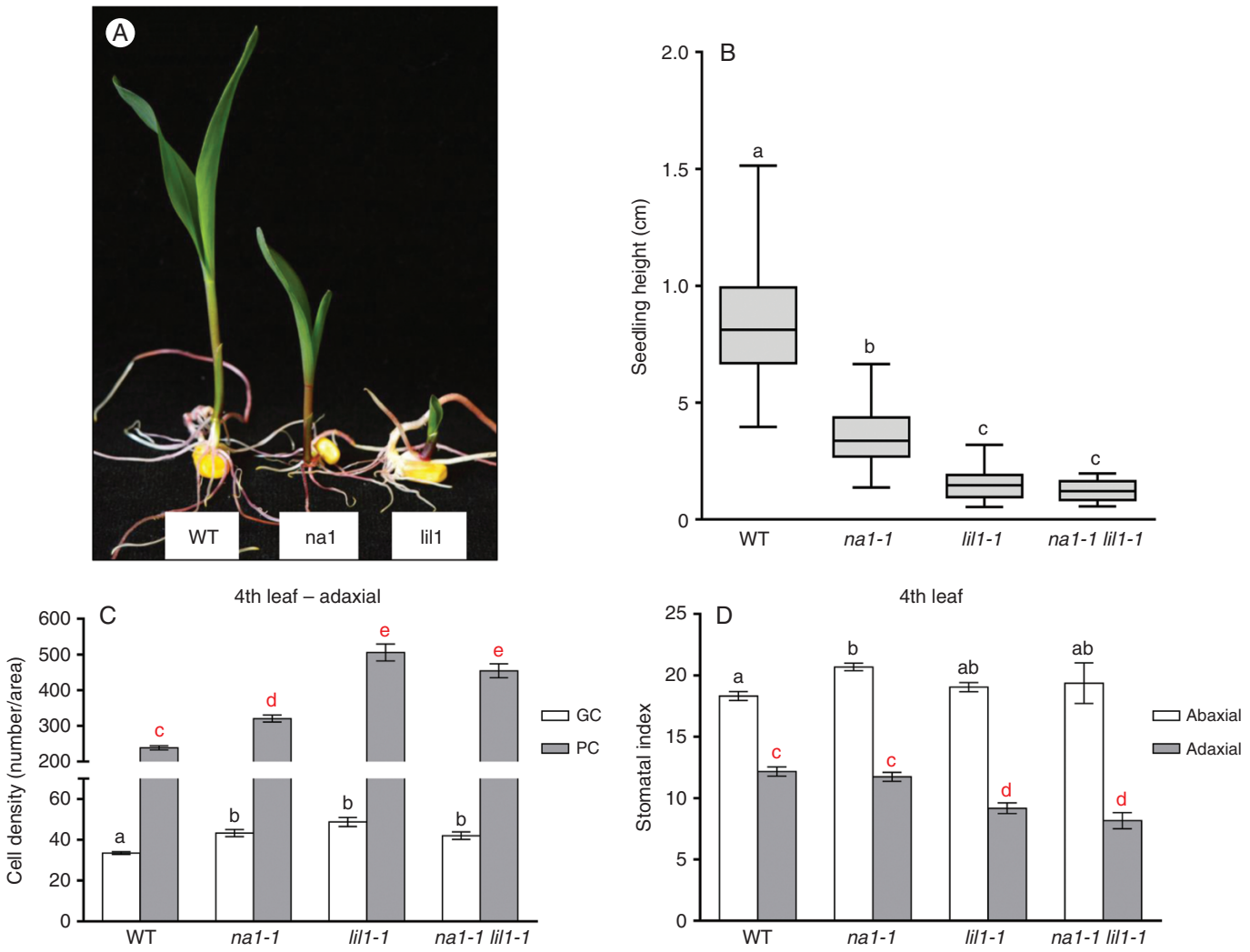

FIG. 3. The *lil1-1* mutant is epistatic to the *na1-1* mutant . (A) Representative wild-type (WT), na1-like (na1) and lil1-like (lil1) phenotypes of 10-day old F_2 plants obtained from selfing F_1 heterozygous *na1-1*/+ *lil1-1*/+ plants. (B–D) Characterization of WT, homozygous *na1-1*, homozygous *lil1-1* and double-homozygous *na1-1 lil1-1* genotypic classes. (B) Whisker plot representing seedling height of 10-day old plants. (C) Numbers of guard cells (GC) and pavement cells (PC). (D) Stomatal index of fourth fully expanded leaves of 50-day old plants. Error bars show the standard error. In (B), (C) and (D) different letters denote differences between values that are statistically significant ($P < 0.05$) as calculated by one-way ANOVA. In (C) GC (black letters) or PC (red letters) values were compared. In (D) abaxial (black letters) or adaxial (red letters) values were compared.

compared with wild-type (Supplementary Data Fig. S3E) and *na1-1* plants (Supplementary Data Fig. S3F).

The adaxial side (Fig. 3C) and the abaxial side (Supplementary Data Fig. S3I) of the fourth leaf presented the same trend, but in the first the differences in PC density between the mutant and wild-type plants was higher. The resulting stomatal index (Fig. 3D) revealed statistically significant differences only in the adaxial side (grey); wild-type and *na1-1* plants were identical, while *lil1-1* and double *lil1-1 na1-1* mutants had similar values to each other but differed from the first two.

The stomatal index (Supplementary Data Fig. S3J) and cell density (Supplementary Data Fig. S3K, L) were also analysed for the adaxial and abaxial sides of the sixth leaf. The results were consistent for the fourth and the sixth leaves and both surfaces.

The lil1-1 *plants showed altered leaf permeability and cuticular wax deposition*

We observed that *lil1-1* seedling leaves were thicker than wild-type leaves (Fig. 2C) and had crinkly sectors on their surfaces. To assess the effect of the mutations on leaf permeability a chlorophyll-leaching assay was performed and showed that chlorophyll was more readily released from wild-type leaves than from mutant ones, thus indicating that BR reduction leads to a decrease in leaf permeability. Similar behaviour was observed for both *lil1-1* and *na1-1* mutants during the assay (Fig. 4A).

Further analyses were then conducted for the *lil1-1* mutant to test the involvement of cuticle changes in the altered morphology and permeability. We first observed that mutant leaves, unlike wild-types leaves, retained water beads on their surface

when they were misted with water (Fig. 4B, C). This was indicative of an alteration in epicuticular waxes, which was indeed highlighted by scanning electron microscopic analysis of the abaxial surface of wild-type and mutant leaves (Fig. 4D–I). Mutant crystalloids appeared less dense, slightly smaller and more embedded in the subtending cuticular material (Fig. 4E, F, H, I) if compared with wild-type ones (Fig. 4D, G).

Homozygous lil1-1 *plants are more tolerant to drought stress*

Cuticular waxes provide a continuous waterproof barrier and protect plant organs against different environmental stresses. They have been shown to be actively involved in reducing leaf passive water loss (Post-Beittenmiller, 1996). On this basis, we compared wild-type and *lil1-1* seedlings for their response to drought stress conditions.

Plants at the fourth-leaf stage grown in pots in well-watered conditions (Fig. 5A) were subjected to drought stress by terminating irrigation. From this time, which was defined as Day 0, soil was allowed to dry progressively. The RSWC, as determined after 3, 6 and 9 days (Fig. 5C), was the same in the two genotypes, thus indicating that the drought stress treatment was identical.

After 6 days without water, we observed that *lil1-1* plants were less damaged than wild types and their leaves remained greener, whereas wild-type plants showed more severe wilting and leaf chlorosis (Fig. 5B). In addition, measurement of leaf RWC, a marker indicating the balance between intrinsic water supply and transpiration rate, revealed similar values in well-watered conditions, but higher values in mutant than in wild-type plants, 9 days after the cessation of irrigation (Fig. 5D). Taken together, these observations indicated that *lil1-1* mutant plants have better tolerance to water stress.

Physiological parameters were assayed at Day 0 (well-watered plants) and after 3 and 4 days of drought treatment and comparisons were made between wild-type and *lil1-1* values at each time point. Measurements of stomatal conductance (g_s) and transpiration rate (E) showed higher mean values in mutant than in wild-type plants at the same developmental stage under drought stress (Fig. 5E, F). Similarly, net photosynthesis rate (A), which had the same values in the two genotypes at Day 0, showed a higher level in mutants under drought stress. Wild types showed low and negative values at 3 and 4 days of drought, respectively (Fig. 5G). In wild types, the high intercellular CO_2 concentration (C_i) measured at 4 days probably indicated almost complete stomatal closure, whereas in mutants the constant C_i values suggested that they maintain their stomata slightly open and functional even during drought treatment (Supplementary Data Fig. S4A). Despite this, mutants deprived of water for 4 days could maintain water use efficiency (WUE) at a constant level, whereas wild types had a negative value for this parameter (Supplementary Data Fig. S4B).

A subset of plants (40 plants per genotype) subjected to water stress was then re-watered. After 3 and 7 days from the starting of re-watering, plants were classified in three categories: (1) severely wilted; (2) slightly wilted; and (3) recovered (Supplementary Data Fig. S4C–I). The percentage of plants showing complete recovery (category 3) was higher in mutant than wild-type plants (Supplementary Data Fig. S4I). The recovery assay indicated that, upon rehydration, mutant plants have a more rapid response, and this confirms their dehydration tolerance.

DISCUSSION

The *lil1-1* mutant, isolated from an active *Mu* population, shows a drastic reduction in plant growth (Dolfini *et al.*, 1999). The molecular and genetic analysis carried out in this study disclosed that the lil1 phenotype is due to a *Mu1* insertion in the second exon of the maize *cytochrome P450 CYP85A1 C-6 oxidase* gene, which is involved in the last steps of the BR pathway. *lil1-1* is allelic to the previously isolated *brd1-m1* (Makarevitch *et al.*, 2012; Fig. 1; Supplementary Data Table S1).

The phenotype of *lil1-1* plants appears more severe than that of the other BR-related mutants so far isolated in maize, such as *na1-1* (Hartwig *et al.*, 2011). Analysis of F_2 progenies segregating for both *lil1-1* and *na1-1* mutants revealed that *lil1* is epistatic to *na1*. The product of *na1*, which is the maize orthologue of *A. thaliana DET2*, is a 5α-reductase located further upstream in the BR pathway, which catalyses multiple steps in different branches of the pathway. Our data suggest the existence in the maize BR pathway of an additional *na1*-independent branch leading to the production of CS precursors. Accordingly, CS, although detected at a reduced concentration, was not completely absent in *na1* mutants (Hartwig *et al.*, 2011).

We show in this study that *lil1* gene action is involved in different aspects of plant development but is not required for seed development. Many reports have highlighted the importance of BRs in seed development in different species (Vriet *et al.*, 2012; Jiang and Lin, 2013). In arabidopsis, seeds of the BR-deficient mutant *det2* and the BR-insensitive mutant *bri1-5* are smaller compared with wild-type seeds (Jiang *et al.*, 2013). Similarly, the rice BR-deficient mutants *brd2* (Hong *et al.*, 2005) and dwarf mutant *d61* (Morinaka *et al.*, 2006) have shortened and smaller grains. In contrast, we did not find any obvious phenotypic variations related to seed development and seed weight in homozygous *lil1-1* mutant compared with wild-type kernels (Supplementary Data Table S2). However, in the aforementioned studies, mutant seeds were produced by homozygous mutant plants. The observed variations in seed size and production could therefore be attributed to alterations in the BR level of the mother plant. This was observed in transgenic rice plants, in which the BR level was altered only in the stems, leaves and roots and not in seeds. Changes in plant architecture had an impact on seed production, which was higher in transgenic than in the control wild-type plants (Wu *et al.*, 2008). In our work, comparisons were among seeds produced by wild-type plants. We assumed that mother plants had a normal BR level and concluded that the *lil1-1* mutation does not have an effect on seed size and production.

Comparison of *lil1-1* mutant and wild-type seedlings soon after germination highlighted defective primary root growth. In germinating seeds, wild-type primary roots exhibited a downward curvature, whereas homozygous *lil1-1* roots grew either parallel to the surface or with an upward orientation (Fig. 2E, F). Brassinosteroid hormones were detected in root tissues in maize (Kim *et al.*, 2000) as well as in arabidopsis and tomato (Yokota *et al.*, 2001; Bancos *et al.*, 2002). In maize, the work

of Kim *et al.* (2000) also showed that exogenous application of different BRs, including CS and BL, stimulated the gravitropic response. A positive influence of BL on root curvature was also observed in *Pisum sativum* (Amzallag and Vaisman, 2006), and in arabidopsis, in which BR signalling mutants exhibited a reduced gravitropic curvature, whereas transgenic plants over-expressing BRI1 displayed a greater gravitropic curvature than wild-type plants (Kim *et al.*, 2007).

The present work provides the first genetic evidence of BR involvement in gravitropic curvature in maize. Positive gravitropic movement normally occurs in response to the stimulus of gravity and causes a downward curvature of the root. Beside BRs, the plant hormones auxin and ethylene exert a stimulatory role on the root gravitropic response in maize (Kim *et al.*, 2000; Chang *et al.*, 2004). A model has been proposed to explain their roles, in which BL promotes the gravitropic response by stimulating auxin-induced ethylene production (Chang *et al.*, 2004). The higher level of ethylene would lead to an increase in gravitropic curvature. A different pathway might also be implicated in this response, since gravity perception and signal transduction are also stimulated by BL in a way independent of ethylene (Chang *et al.*, 2004). A deeper characterization of BR-deficient

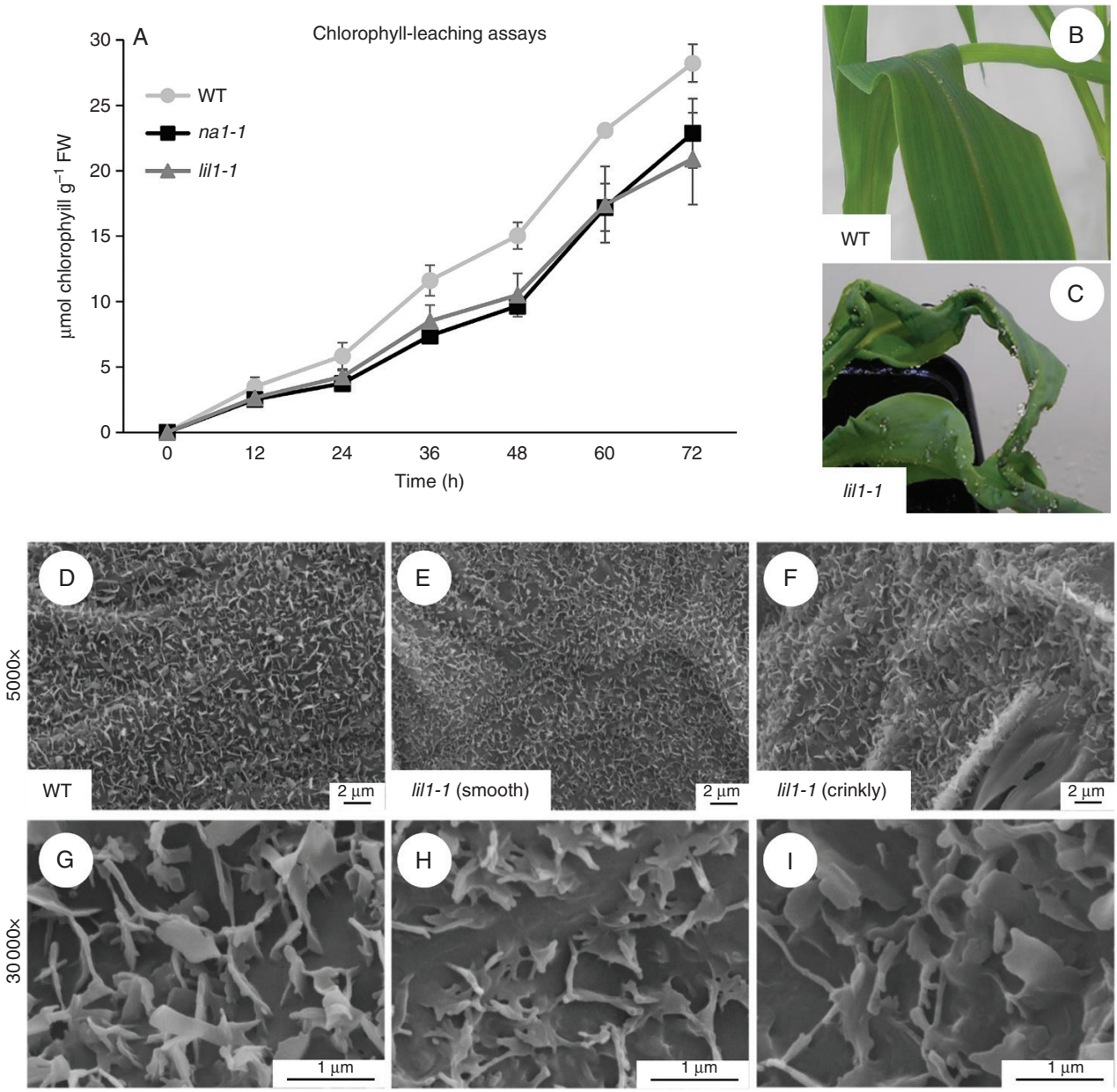

FIG. 4. Permeability and cuticular wax analysis. (A) Chlorophyll leaching assay on the sixth fully expanded leaf of 40-day old wild-type (WT), homozygous *na1-1* and homozygous *lil1-1* mutant plants. Values represent the mean of five leaves per genotype. Error bars show the standard error. FW, fresh weight. (B, C) Representative adult leaf phenotype of WT (B) and homozygous *lil1-1* mutant (C) plants misted with water. (D–I) Scanning electron microscope images of epicuticular waxes of the fourth adaxial leaf surface of WT (D, G) and homozygous *lil1-1* mutant plants (E, F, H, I). Mutant samples were taken from a smooth (E, H) and a crinkly sector (F, I) of the leaf.

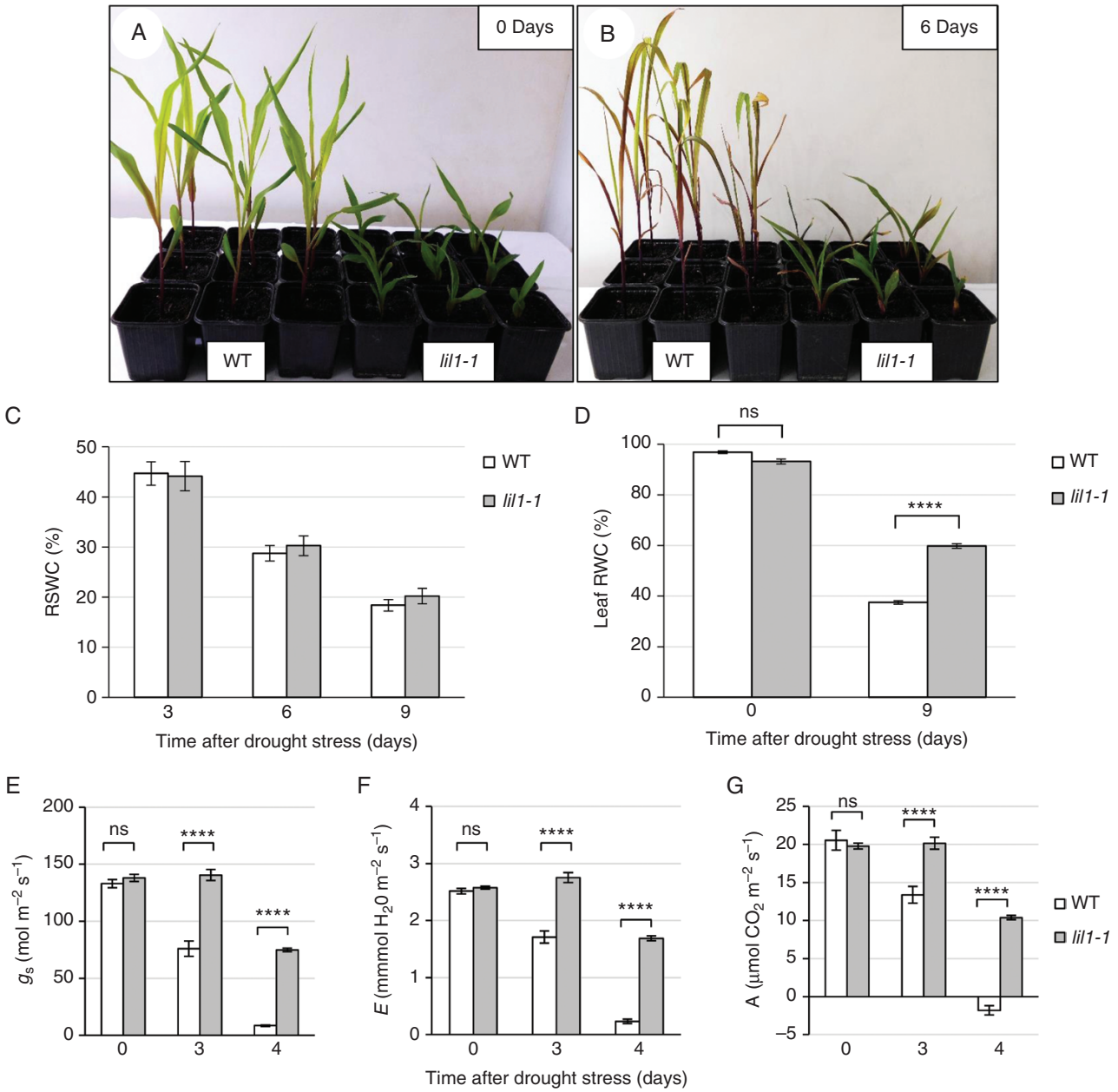

FIG. 5. The *lil1-1* mutant plants are more tolerant to drought stress. (A) Representative phenotype of 14-day old wild-type (WT) and homozygous *lil1-1* mutant plants grown under well-watered conditions (0 Days) and (B) after 6 days of drought stress initiation by withholding irrigation (6 Days). (C) Relative soil water content (RWSC) measured at 0, 3, 6 and 9 days after drought stress indicates that the water loss from the soil of pots in which WT plants were grown was identical to that of pots in which mutant (*lil1*-1) plants were grown. (D) Leaf relative water content (RWC) of WT and homozygous *lil1-1* mutant plants at 0 and 9 days of drought treatment. (E, F) Physiological parameters were measured at 0, 3 and 4 days. (E) Stomatal conductance (g_s). (F) Transpiration rate (*E*). (G) Net photosynthesis rate (*A*). Error bars in (C–G) show standard error. Comparison was made at each time point between wild-type and homozygous *lil1-1* genotypes. ****$P < 0.0001$ (two tailed Student's *t*-test); ns, not significant.

mutants like *lil1-1* will allow a better comprehension of the process.

Many studies have shown that plant tolerance to drought stress is increased by exogenous application of BRs (Krishna, 2003; Bajguz and Hayat, 2009). However, the analyses in various species of mutants with reduced endogenous levels and/or perception of these hormones seems to lead to contrasting conclusions. In *A. thaliana*, reduced BR accumulation, due to either loss of CYP85A2 activity or CYP85A farnesylation, increased drought tolerance (Northey *et al.*, 2016). Higher tolerance to both salt and drought stresses was also observed in the loss-of-function *gsk1* mutant carrying a T-DNA insertion in the rice orthologue of the *A. thaliana BIN2* (*BR-INSENSITIVE 2*) gene (Koh *et al.*, 2007). In the same species, the *d1* mutant, carrying a mutation in the *RGA1* gene involved in both Gibberellin (GA) and BR signalling, showed reduced sensitivity to drought (Ferrero-Serrano and Assman, 2016). RNAi mutants of the *Brachypodium distachyon BdBRI1* gene, encoding the BR

receptor, exhibited enhanced drought tolerance, accompanied by high expression of drought-responsive genes (Feng *et al.*, 2015). Similarly, in our study we show that *lil1-1* mutant plants were better adapted to drought stress conditions. Moreover, recovery from stress conditions occurred more rapidly in mutant than in wild-type plants (Supplementary Data Fig. S4), an observation that was also reported for the mutant in the *BdBRI1* gene (Feng *et al.*, 2015).

This behaviour might be due to a better capacity of mutant plants to retain water, as shown by the analysis of leaf RWC, which was significantly higher in mutants after the cessation of irrigation (Fig. 5D; Feng *et al.*, 2015). We propose that morphological changes, such as leaf thickness (Fig. 2C), lower stomatal index (Fig. 3D, Supplementary Data Fig. S3J) and altered epicuticular waxes (Fig. 4) may improve water retention by mutant leaves. In agreement with this, the chlorophyll leaching assay showed that permeability was lower in mutant than in wild-type leaves.

It has been shown in barley that drought causes a significant increase in the accumulation of biologically active BR molecules (Gruszka *et al.*, 2016). In addition, an interesting hypothesis suggests that alteration in BR level induces the presence, by default, of a physiological stress condition. The activity of oxidative stress-related genes, including cold and drought stress response genes and heat stress-related genes, was shown to be enhanced in BR-deficient plants. In the arabidopsis *bri1-9* mutant the transcript level of stress-inducible genes and of transcription factors that regulate their expression was constitutively higher in comparison with wild types (Kim *et al.*, 2010). This condition may confer a higher capacity to respond to and tolerate stresses. Of interest in this context is the study of the *det2* mutant showing enhanced resistance to general oxidative stress, in which the *ATPA2* and *ATP24a* genes, encoding peroxidases, were constitutively upregulated (Goda *et al.*, 2002; Shuqing *et al.*, 2005). Analogies between *lil1-1* and *det2* phenotypic traits, such as thicker leaves, thicker cuticle and increased guard cell density, suggest that the two mutants share the same type of response. Further investigation is needed to unravel the molecular mechanisms by which BRs influence drought stress response in maize. It is conceivable that new information arising from these studies will allow us to establish novel manipulation approaches aimed at improving crop adaptability to environmental stress.

CONCLUSIONS

We show in this study that the characterization of mutants with deficiency in BR accumulation and the analysis of their interactions are instrumental in improving our knowledge of the architecture of the pathway in maize. Detailed mutant analysis has also been instrumental in highlighting novel developmental processes in which these hormones are involved. In addition, we provide the first evidence in maize that BRs play a role in the plant response to drought. Although further studies are required to clarify the molecular mechanisms at the basis of the BR-mediated response, this may offer a possible direction to future breeding programmes aimed at improving crop adaptation to changes in climate and environmental conditions.

SUPPLEMENTARY DATA

Supplementary data are available online at www.aob.oxfordjournals.org and consist of the following. Figure S1: the *Mu1* insertion within the maize *CYP85A1* gene co-segregates with the lil1 mutant phenotype. Figure S2: both *lil1-1* and *brd1-m1* mutants showed reduced plant size. Figure S3: phenotypic and morphological analysis of F_2 progeny plants obtained from selfing double-heterozygous *na1-1*/+ *lil1-1*/+ plants. Figure S4: recovery from drought stress. Table S1: allelism test. Table S2: seed weight is not affected by the *lil1-1* mutation. Table S3: mother plant genotype does not affect seed production. Table S4: gravitropic response is altered in the *lil1-1* mutant seedling primary root. Table S5: segregation of seedling phenotypes and genotypes in F_2 progeny obtained from selfing double-heterozygous plants. Table S6: PCR primers used in this study.

ACKNOWLEDGEMENTS

We wish to thank the Maize Genetics Cooperation Stock Center, Urbana, IL, USA for sending the *na1-1* and *brd1-m1* stocks, Dr Nadia Santo at the Biosciences Imaging Facility (University of Milan) for the analysis with the scanning electron microscope and Dr Lesley Currah for editing the manuscript.

LITERATURE CITED

Amzallag GN, **Vaisman J. 2006**. Influence of brassinosteroids on initiation of the root gravitropic response in *Pisum sativum* seedlings. *Biologia Plantarum* **50**: 283–286.

Arthur K, **Vejlupkova Z**, **Meeley R**, **Fowler J. 2003**. Maize ROP2 GTPase provides a competitive advantage to the male gametophyte. *Genetics* **165**: 2137–2151.

Bajguz A, **Hayat S. 2009**. Effects of brassinosteroids on the plant responses to environmental stresses. *Plant Physiology and Biochemistry* **47**: 1–8.

Bancos S, **Nomura T**, **Sato T**, ***et al.* 2002**. Regulation of transcript levels of the *Arabidopsis* cytochrome P450 genes involved in brassinosteroid biosynthesis. *Plant Physiology* **130**: 504–513.

Best NB, **Hartwig T**, **Budka J**, ***et al.* 2016**. *nana plant2* encodes a maize ortholog of the *Arabidopsis* brassinosteroid biosynthesis protein Dwarf1, identifying developmental interactions between brassinosteroids and gibberellins. *Plant Physiology* **171**: 00399.

Bishop GJ, **Harrison K**, **Jones JD. 1996**. The tomato *Dwarf* gene isolated by heterologous transposon tagging encodes the first member of a new cytochrome P450 family. *Plant Cell* **8**: 959–969.

Bishop GJ, **Nomura T**, **Yokota T**, ***et al.* 1999**. The tomato DWARF enzyme catalyses C-6 oxidation in brassinosteroid biosynthesis. *Proceedings of the National Academy of Sciences of the USA* **96**: 1761–1766.

Chang SC, **Kim YS**, **Lee JY**, ***et al.* 2004**. Brassinolide interacts with auxin and ethylene in the root gravitropic response of maize (*Zea mays*). *Physiologia Plantarum* **121**: 666–673.

Choe S, **Dilkes BP**, **Gregory BD**, ***et al.* 1999**. The *Arabidopsis dwarf1* mutant is defective in the conversion of 24-methylenecholesterol to campesterol in brassinosteroid biosynthesis. *Plant Physiology* **119**: 897–907.

Clouse SD. 2011. Brassinosteroid signal transduction: from receptor kinase activation to transcriptional networks regulating plant development. *Plant Cell* **23**: 1219–1230.

Divi UK, **Krishna P. 2009**. Brassinosteroid: a biotechnological target for enhancing crop yield and stress tolerance. *New Biotechnology* **26**: 131–136.

Dolfini S, **Landoni M**, **Consonni G**, **Rascio N**, **Dalla Vecchia F**, **Gavazzi G. 1999**. The maize *lilliputian* mutation is responsible for disrupted morphogenesis and minute stature. *Plant Journal* **17**: 11–17.

Feng Y, **Yin Y**, **Feia S. 2015**. Down-regulation of BdBRI1, a putative brassinosteroid receptor gene produces a dwarf phenotype with enhanced drought tolerance in *Brachypodium distachyon*. *Plant Science* **234**: 163–173.

Ferrero-Serrano Á, **Assmann SM**, **2016**. The α-subunit of the rice heterotrimeric G protein, RGA1, regulates drought tolerance during the vegetative phase in the dwarf rice mutant *d1*. *Journal of Experimental Botany* **67**: 3433–3443.

Goda H, **Shimada Y**, **Asami T**, **Fujioka S**, **Yoshida S. 2002**. Microarray analysis of brassinosteroid-regulated genes in *Arabidopsis*. *Plant Physiology* **130**: 1319–1334.

Gruszka D, **Janeczko A**, **Dziurka M**, **Pociecha E**, **Oklestkova J**, **Szarejko I. 2016**. Barley brassinosteroid mutants provide an insight into phytohormonal homeostasis in plant reaction to drought stress. *Frontiers in Plant Science* **7**: 1824.

Gutiérrez-Marcos JF, **Dal Prà M**, **Giulini A**, ***et al.*** **2007**. *empty pericarp4* encodes a mitochondrion-targeted pentatricopeptide repeat protein necessary for seed development and plant growth in maize. *Plant Cell* **19**: 196–210.

Hartwig T, **Chuck GS**, **Fujioka S**, ***et al.*** **2011**. Brassinosteroid control of sex determination in maize. *Proceedings of the National Academy of Sciences of the USA* **108**: 19814–19819.

Hong Z, **Ueguchi-Tanaka M**, **Fujioka S**, ***et al.*** **2005**. The rice brassinosteroid-deficient dwarf2 mutant, defective in the rice homolog of *Arabidopsis* DIMINUTO/DWARF1, is rescued by the endogenously accumulated alternative bioactive brassinosteroid, dolichosterone. *Plant Cell* **17**: 2243–2254.

Janeczko A, **Gruszka D**, **Pociecha E**, ***et al.*** **2016**. Physiological and biochemical characterisation of watered and drought-stressed barley mutants in the *HvDWARF* gene encoding C6-oxidase involved in brassinosteroid biosynthesis. *Plant Physiology and Biochemistry* **99**: 126–141.

Jiang WB, **Lin WH. 2013**. Brassinosteroid functions in *Arabidopsis* seed development. *Plant Signaling & Behavior* **8**: e25928.

Jiang WB, **Huang HY**, **Hu YW**, **Zhu SW**, **Wang ZY**, **Lin WH. 2013**. Brassinosteroid regulates seed size and shape in *Arabidopsis*. *Plant Physiology* **162**: 1965–1977.

Kim BK, **Fujioka S**, **Takatsuto S**, **Tsujimoto M**, **Choe S. 2008**. Castasterone is a likely end product of brassinosteroid biosynthetic pathway in rice. *Biochemical and Biophysical Research Communications* **374**: 614–619.

Kim S-K, **Chang SC**, **Lee EJ**, ***et al.*** **2000**. Involvement of brassinosteroids in the gravitropic response of primary root of maize. *Plant Physiology* **123**: 997–1004.

Kim SY, **Kim BH**, **Lim CJ**, **Lim CO**, **Nam KH. 2010**. Constitutive activation of stress-inducible genes in a brassinosteroid-insensitive 1 (bri1) mutant results in higher tolerance to cold. *Plant Physiology* **138**: 191–204.

Kim TW, **Lee SM**, **Joo SH**, ***et al.*** **2007**. Elongation and gravitropic responses of *Arabidopsis* roots are regulated by brassinolide and IAA. *Plant, Cell & Environment* **30**: 679–689.

Kir GYH, **Nelissen H**, **Neelakandan AK**, ***et al.*** **2015**. RNA interference knockdown of BRASSINOSTEROID INSENSITIVE1 in maize reveals novel functions for brassinosteroid signaling in controlling plant architecture. *Plant Physiology* **169**: 826–839.

Koh S, **Lee SC**, **Kim MK**, ***et al.*** **2007**. T-DNA tagged knockout mutation of rice *OsGSK1*, an orthologue of *Arabidopsis BIN2*, with enhanced tolerance to various abiotic stresses. *Plant Molecular Biology* **65**: 453–466.

Krishna P. 2003. Brassinosteroid-mediated stress responses. *Journal of Plant Growth Regulation* **22**: 289–297.

Li J, **Nagpal P**, **Vitart V**, **McMorris TC**, **Chory J. 1996**. A role for brassinosteroids in light-dependent development of *Arabidopsis*. *Science* **272**: 398–402.

Lolle SJ, **Berlyn GP**, **Engstrom EM**, **Krolikowski KA**, **Reiter W. 1997**. Developmental regulation of cell interactions in the *Arabidopsis* fiddlehead-1 mutant: a role for the epidermal cell wall and cuticle. *Developmental Biology* **321**: 311–321.

Makarevitch I, **Thompson A**, **Muehlbauer GJ**, **Springer NM. 2012**. *Brd1* gene in maize encodes a brassinosteroid C-6 oxidase. *PloS ONE* **7**: e30798.

Morinaka Y, **Sakamoto T**, **Inukai Y**, ***et al.*** **2006**. Morphological alteration caused by brassinosteroid insensitivity increases the biomass and grain production of rice. *Plant Physiology* **141**: 924–931.

Northey JGB, **Liang S**, **Jamshed M**, ***et al.*** **2016**. Farnesylation mediates brassinosteroid biosynthesis to regulate abscisic acid responses. *Nature Plants* **2**: 1–7.

Nomura T, **Kushiro T**, **Yokota T**, **Kamiya Y**, **Bishop GJ**, **Yamaguchi S. 2005**. The last reaction producing brassinolide is catalyzed by cytochrome P-450s, CYP85A3 in tomato and CYP85A2 in *Arabidopsis*. *Journal of Biology Chemistry* **280**: 17873–17879.

Pérez-España VH, **Sánchez-León N**, **Vielle-Calzada JP. 2011**. CYP85A1 is required for the initiation of female gametogenesis in *Arabidopsis thaliana*. *Plant Signaling & Behavior* **6**: 321–326.

Pieczynski M, **Marczewski W**, **Hennig J**, ***et al.*** **2013**. Down-regulation of *CBP80* gene expression as a strategy to engineer a drought-tolerant potato. *Plant Biotechnology Journal* **11**: 459–469.

Post-Beittenmiller D. 1996. Biochemistry and molecular biology of wax production in plants. *Annual Review of Plant Biology* **47**: 405–430.

La Rocca N, **Manzotti PS**, **Cavaiuolo M**, ***et al.*** **2015**. The *maize fused leaves1* (*fdl1*) gene controls organ separation in the embryo and seedling shoot and promotes coleoptile opening. *Journal of Experimental Botany* **66**: 5753–5767.

Shimada Y, **Fujioka S**, **Miyauchi N**, ***et al.*** **2001**. Brassinosteroid-6- oxidases from *Arabidopsis* and tomato catalyze multiple C-6 oxidations in brassinosteroid biosynthesis. *Plant Physiology* **126**: 770–779.

Shuqing C, **Qiaoting X**, **Yajun C**, ***et al.*** **2005**. Loss-of-function mutations in DET2 gene lead to an enhanced resistance to oxidative stress in *Arabidopsis*. *Physiologia Plantarum* **123**: 57–66.

Vriet C, **Russinova E**, **Reuzeau C. 2012**. Boosting crop yields with plant steroids. *Plant Cell* **3**: 842–857.

Wu C, **Trieu A**, **Radhakrishnan P**, ***et al.*** **2008**. Brassinosteroids regulate grain filling in rice. *Plant Cell Online* **20**: 2130–2145.

Yokota T, **Sato T**, **Takeuchi Y**, ***et al.*** **2001**. Roots and shoots of tomato produce 6-deoxo-28-norcathasterone, 6-deoxo-28-nortyphasterol and 6-deoxo-28-norcastasterone, possible precursors of 28-norcastasterone. *Phytochemistry* **58**: 233–238.